INSTITUT DE FRANCE
Académie des sciences

Comptes Rendus

Physique

Alaska Subedi

Light-control of materials via nonlinear phononics

Volume 22, Special Issue S2 (2021), p. 161-184

Published online: 26 March 2021
Issue date: 3 December 2021

https://doi.org/10.5802/crphys.44

Part of Special Issue: Physics of ultra-fast phenomena
Guest editors: Éric Collet (Université Rennes 1, CNRS, France) and Sylvain Ravy (Université Paris-Saclay, CNRS, France)

Les Comptes Rendus. Physique *sont membres du*
Centre Mersenne pour l'édition scientifique ouverte
www.centre-mersenne.org
e-ISSN : 1878-1535

Comptes Rendus
Physique
2021, 22, nº S2, p. 161-184
https://doi.org/10.5802/crphys.44

Physics of ultra-fast phenomena / *Physique des phénomènes ultra-rapides*

Light-control of materials via nonlinear phononics

Alaska Subedi [a, b]

[a] CPHT, CNRS, Ecole Polytechnique, IP Paris, F-91128 Palaiseau, France

[b] Collège de France, 11 place Marcelin Berthelot, 75005 Paris, France

E-mail: alaska.subedi@polytechnique.edu

Abstract. Nonlinear phononics is the phenomenon in which a coherent dynamics in a material along a set of phonons is launched after its infrared-active phonons are selectively excited using external light pulses. The microscopic mechanism underlying this phenomenon is the nonlinear coupling of the pumped infrared-active mode to other phonon modes present in a material. Nonlinear phonon couplings can cause finite time-averaged atomic displacements with or without broken crystal symmetries depending on the order, magnitude and sign of the nonlinearities. Such coherent lattice displacements along phonon coordinates can be used to control the physical properties of materials and even induce transient phases with lower symmetries. Light-control of materials via nonlinear phononics has become a practical reality due to the availability of intense mid-infrared lasers that can drive large-amplitude oscillations of the infrared-active phonons of materials. Mid-infrared pump induced insulator–metal transitions and spin and orbital order melting have been observed in pump–probe experiments. First principles based microscopic theory of nonlinear phononics has been developed, and it has been used to better understand how the lattice evolves after a mid-infrared pump excitation of infrared-active phonons. This theory has been used to predict light-induced switching of ferroelectric polarization as well as ferroelectricity in paraelectrics and ferromagnetism in antiferromagnets, which have been partially confirmed in recent experiments. This review summarizes the experimental and theoretical developments within this emerging field.

Keywords. Nonlinear phononics, Ultrafast control, Light-matter interaction, Mode-selective control, Light-induced phonon dynamics.

Available online 18th March 2021

1. Introduction

Light is a popular probe that is widely used to investigate the structure and properties of materials. However, light has seldom been used to coherently control materials, notwithstanding its use as a source of heat. New methods for modifying crystal structures can lead to previously unexplored structures with unusual physical properties. Therefore, there is much interest in developing a technique to control materials using light in the hope that this can be used to stabilize hitherto unknown structures that have not been accessed using pressure, heterostructuring or isovalent chemical doping.

On the practical side, light-control of materials requires intense laser sources that excite materials and examine the excited state. Such pump–probe laser setups were pioneered in chemistry laboratories, and their development was instigated by the dream of controlling chemical reactions by selectively exciting bond-specific vibrations using ultrashort laser pulses [1]. In a thermodynamically activated chemical reaction, statistical laws imply that indiscriminately imparted energy to the reactants cause large amplitude atomic vibrations along the weak bonds, which then get ruptured. By using an intense laser pulse to induce large amplitude vibrations along a stronger bond-stretching mode, it has been shown that it is possible to modify the chemical reaction pathway and obtain a different set of products [2]. However, bond-selective light-control of chemical reactions has only been successful in relatively simple molecules with few atoms [3]. In complex molecules, it has been found that the vibrational energy in the pumped mode is quickly redistributed to other modes present in the molecule, and the pumped mode dissipates and dephases before the amplitude of its vibration becomes large [4].

Vibrational energy redistribution occurs due to nonlinear couplings between the vibrational modes of a molecule [5, 6]. Two-dimensional (2D) pump–probe spectroscopy techniques have been developed that can simultaneously measure the oscillations of the pumped mode and other modes that are nonlinearly coupled to it [7]. This has allowed the determination of the nature and magnitude of the nonlinear couplings, as well as the dissipation and dephasing times of the vibrations. The nonlinear couplings between different vibrational modes appear as off-diagonal peaks in 2D pump–probe spectroscopy measurements. In addition to the lowest-order $Q_1 Q_2$ coupling between two vibrational mode coordinates Q_1 and Q_2, higher-order $Q_1 Q_2^2$ nonlinearity has also been inferred from the measurements [8, 9]. It has also been noted that $Q_1 Q_2^2$ nonlinearity causes Frank–Condon-like displacement along the vibrational coordinates in the excited state [10].

Although nonlinear couplings between vibrational modes are an impediment to bond-selective chemistry in large molecules, they do lead to observation of coherent vibrations of nonlinearly coupled modes in 2D pump–probe spectroscopy. The discussion of a similar effect in crystalline solids due to nonlinear coupling between phonons starts with the proposal of ionic Raman scattering in the 1970s [11, 12]. These studies showed that infrared-active (IR-active) phonons can play the role of an intermediate state in a Raman scattering process in the presence of a $Q_{\mathrm{R}} Q_{\mathrm{IR}}^2$ nonlinear coupling between a Raman-active phonon mode Q_{R} and an IR-active phonon mode Q_{IR}.

Ionic Raman scattering has not yet been observed in light scattering experiments. However, Först *et al.* observed coherent oscillations at frequencies corresponding to Raman-active phonon modes in their time-resolved reflectivity measurements after a mid-IR pump in metallic $La_{0.7}Sr_{0.3}MnO_3$ [13]. They proposed that these oscillations occur because Raman-active modes are coherently excited when an IR-active phonon mode is externally pumped due to $Q_{\mathrm{R}} Q_{\mathrm{IR}}^2$ nonlinearities, and this phenomenon has been called stimulated ionic Raman scattering. In that study, oscillations of the pumped mode were not measured via time-resolved spectroscopy experiments to show that IR-active phonon excitations, and not electronic excitations, are responsible for the coherent oscillations of the Raman-active phonons. However, coherent oscillations at Raman-active phonon frequencies have been observed in insulating $ErFeO_3$ [14] and $LaAlO_3$ [15] in time-resolved spectroscopy experiments after a mid-IR pump, and these experiments do show that the amplitude of the oscillations are largest when the pump frequency is tuned to the frequency of the IR-active phonon mode. Moreover, oscillations of the pumped mode as well as the nonlinearly coupled low-frequency mode have been simultaneously observed after a mid-IR pump in time-resolved second harmonic generation (SHG) experiment on $LiNbO_3$ [16], which conclusively demonstrates the phenonmenon of stimulated ionic Raman scattering.

Först *et al.* have also noted that a Raman-active phonon mode experiences a force proportional to gQ_{IR}^2 in the presence of a nonlinear coupling term $gQ_{\mathrm{R}}Q_{\mathrm{IR}}^2$ with coupling constant g [13]. Since the force is proportional to the square of the IR-active phonon coordinate, total force exerted on the Raman-active mode has a nonzero time-averaged value while the IR-active mode is oscillating. This causes the lattice to get displaced along the Raman-active phonon coordinate when the IR-active mode is pumped, and this phenonmena has been termed nonlinear phononics. Time-resolved X-ray diffraction experiments on $La_{0.7}Sr_{0.3}MnO_3$ and $YBa_2Cu_3O_{6.5}$ after an intense mid-IR excitation have found intensity modulation of Bragg peaks of less than 0.5%, and it has been argued that these modulations are due to lattice displacement along Raman-active phonon coordinates [17, 18]. In $YBa_2Cu_3O_{6.5}$, this corresponds to bond length changes of less than 1 pm. Furthermore, these materials are metallic, and oscillations of the pumped mode have not been measured in these experiments to rule out electronic excitation as a cause of the structural changes. More convincing evidence of light-induced displacement due to nonlinear phononics has been proposed [19] and then observed in ferroelectric $LiNbO_3$, which has a high-frequency IR-active phonon with a large oscillator strength [16]. In this material, a strong reduction and sign reversal of the electric dipole moment and a simultaneous oscillation at the frequency of the pumped IR-active mode has been observed in pump–probe SHG experiments. This demonstrates that a coherent displacement of the lattice along a phonon coordinate is feasible at least in insulators that have IR-active phonons with a large oscillator strength.

Coherent lattice displacements due to nonlinear phononics after mid-IR excitations have been attributed to be the cause of insulator–metal transitions in $Pr_{1-x}Ca_xMnO_3$ ($x = 0.3, 0.5$) [20, 21] and $NdNiO_3$ [22], orbital order melting in $La_{0.5}Sr_{1.5}MnO_3$ [23, 24], and magnetic order melting in $NdNiO_3$ [25]. Although phase transitions in these materials occur after a mid-IR pump, neither coherent lattice displacements nor excitations of the pumped IR-active phonon was demonstrated in any of these experiments. Therefore, it is not yet known if lattice displacements due to nonlinear phononics can be large enough to modify the physical properties of materials. Most of the currently reported phase transitions due to mid-IR excitations involve melting of order. Since light pulses always impart heat, it may be infeasible to unambiguously show that melting of order is due to nonlinear phononics because it might not be possible to disentangle the effects of heating and light-induced phonon excitations. Light-control of materials properties via nonlinear phononics can only be conclusive when it involves breaking of symmetries that are present in the equilibrium phase. Light-induced breaking of inversion symmetry in oxide paraelectrics has been theoretically predicted [26], and Nova *et al.* have observed metastable ferroelectricity in $SrTiO_3$ after a mid-IR pump [27]. However, the same effect in $SrTiO_3$ has also been achieved using terahertz pump [28]. So it is not yet clear if the observed mid-IR pump induced ferroelectricity is caused by lattice displacements due to nonlinear phononics.

Mid-IR pump terahertz probe experiments have been performed on several superconductors [29–32]. The reflected electric field transients of probe pulses are enhanced by a few percent in these experiments, and the nonequilibrium state with enhanced reflectivity relaxes to the normal state within 1–2 ps. Although the low-frequency optical conductivity of a short-lived state is not a well defined quantity, the Fourier transform of the reflected electric field transients have been analyzed in terms of frequency-domain optical conductivity. The increased time-dependent reflectivity after a mid-IR pump appears as a low-frequency peak in the imaginary part of the reconstructed optical conductivity $\sigma_2(\omega)$, and this has been interpreted as a signature of light-induced superconductivity. In a true superconducting state, the real part of the optical conductivity $\sigma_1(\omega)$ should concomitantly decrease at low frequencies. However, the reconstructed $\sigma_1(\omega)$ shows an increase at low frequencies. Moreover, there have been no two-dimensional spectroscopy experiments to show that an IR-active phonon mode is actually being pumped while the metastable state with increased reflectivity gets transiently realized, making the connection of

nonlinear phononics phenomena in these experiments rather tenuous. In fact, the reconstructed $\sigma_2(\omega)$ shows a superconductivity-like behaviour after a mid-IR pump in samples where even the IR-active phonon is not observed in optical spectroscopy experiments [32], suggesting that the observed light-induced effect is due to electronic excitations. Since light-induced superconductivity is not apparent in the raw data and only manifests after data analysis, this subject will not be discussed in this review. Readers interested in this subject are pointed to reviews that discuss the mid-IR pump experiments in superconductors in detail [33–35].

Light-induced structural dynamics in crystals has been theoretically studied using molecular dynamics [36] and time-dependent density functional theory calculations [37]. These methods have the advantage of taking into account the light-induced changes in all the dynamical degrees of freedom present in the material. But it is cumbersome to extract the relevant nonlinear couplings between the pumped IR-active mode and coupled Raman-active modes from these methods, which hinders the understanding of the microscopic processes that cause the light-induced phenomena. Subedi *et al.* started the use of a theoretical framework to study nonlinear phononics that is based on symmetry principles to identify the symmetry-allowed nonlinear couplings, first principles calculations of the coefficients of these nonlinear terms, and solution of the equations of the motions for the coupled phonon coordinates [38]. This framework was used to explain the light-induced phenonmena observed in the pioneering mid-IR pump experiments in the manganites [13,20]. Calculations based on this framework was used to reconstruct the mid-IR pump-induced changes in the structure of $YBa_2Cu_3O_{6.5}$ [18] and explain the observation of symmetry-breaking Raman-active modes in orthoferrites [39]. A mechanism for ultrafast switching of ferroelectricity was proposed using this method [19], and a recent observation of momentary reversal of ferroeletricity in $LiNbO_3$ has partially confirmed this prediction [16]. Light-induce ferroelectricity [26] and ferromagnetism [40] have also been proposed, the latter prediction based solely on symmetry arguments. Recent mid-IR pump experiments have observed long-lived metastable ferroelectricity in $SrTiO_3$ [27] and ferromagnetism in $DyFeO_3$ [41] and CoF_2 [42], but the precise mechanisms for these phenomena need to be clarified with further experimental studies. Other theoretical predictions based on the nonlinear phonon couplings that await experimental confirmations include indirect-to-direct band gap switching [43], phono-magnetic analogs of opto-magnetic effects [44], cavity control of nonlinear phonon interactions [45], and excitation of an optically silent mode in $InMnO_3$ [46].

Recent successes in light-control of materials using mid-IR pulses show that nonlinear phononics has an important role to play at the frontier of materials physics. This is further underscored by the construction of several free electron laser sources that have recently come online or are in the process of being built. There have been several reviews of this field that have focused on the experimental aspects of the field [33–35, 47–49]. This review attempts to summarize the experimental and theoretical developments in the field of nonlinear phononics, emphasizing how theoretical calculations have helped the experimentalists drive this field forward.

2. Theoretical approach

In nonlinear phononics experiments, experimentalists are equipped with a light source that can strongly excite some set of IR-active phonons of a material, and they want to understand how the structure and physical properties of the material changes after the phonon excitation. In another situation, experimentalists know a phonon mode associated with an order parameter, and they want to identify the IR-active phonons that should be pumped to alter the ordered state by coherently displacing the lattice along the phonon coordinate of the order parameter. Subedi *et al.* initiated the use of a microscopic theory to quantify the nonlinear couplings between the IR- and Raman-active phonons and predict the light-induced structural dynamics from first

principles [38]. This framework relies on (i) symmetry principles to determine which phonon modes can couple to the pumped IR-active phonon, (ii) first principles calculation of the energy surface as a function of the coupled phonon coordinates to extract their nonlinear couplings, and (iii) solution of the coupled equations of motions for the phonon coordinates.

The first step in a nonlinear phononics experiment is the identification of phonons of a material. Since light couples to phonons near the Brillouin zone center, the phonons relevant to a nonlinear phononics experiment are measured using optical reflectivity and Raman scattering experiments. In addition to measuring the frequencies, these experimental methods also yield information about the symmetry of the phonons. In the theory side, density functional theory (DFT) based methods can calculate forces on atoms, and these can be used to construct dynamical matrices. Diagonalization of the dynamical matrices produces phonon frequencies and their irreducible representation (irrep) can be determined by studying how the corresponding eigenvectors transform under the symmetry operations of the point group of the material. In this way, the phonon frequencies and their symmetries can be reconciled between experiment and theory.

The ability to pump a particular set of phonons in a material depends on the frequency and power of the available laser source. The pump-induced response of a material is usually investigated by analyzing the reflected, transmitted or scattered probe pulses. The phonons that are nonlinearly coupled to the pumped IR-active mode are observed as oscillations in the amplitude of the detected probe pulse. Although the response along the coupled phonon modes can easily be detected after a pump, extraction of nonlinear couplings from experimental data has so far proven to be difficult. Additionally, coherent change in lattice can also be inferred from time-resolved diffraction experiments, but a complete determination of the structural changes has been impractical because this requires measuring changes in numerous diffraction peaks as a function of time after a pump. The usefulness of the DFT-based microscopic theory of nonlinear phononics lies in the ability to calculate nonlinear couplings from first principles, which makes it possible to efficiently calculate and predict pump-induced structural changes.

To extract the nonlinear phonon couplings between two modes, the calculated phonon eigenvectors are used to generate a large number of structures as a function of the two phonon coordinates. DFT calculations are run again to calculate total energies of these structures. The total energies are then collected and fit with a polynomial to extract the coefficients corresponding to the nonlinear terms in the expansion of the total energy as a function of the phonon coordinates. Although a generic polynomial can be used to fit the calculated total energy surface, polynomials with only symmetry-allowed terms are used in the fitting to reduce the sources of numerical noise. The symmetry allowed terms are determined by noting that the total energy is a scalar and has the trivial irrep. For the cubic order coupling $Q_{\mathrm{R}}Q_{\mathrm{IR}}^2$, it implies that an IR-active mode can only couple to a Raman mode with the irrep A_g in centrosymmetric crystals because the square of an irrep is the trivial irrep A_g. However, if two different IR modes are pumped simultaneously, then their coupling to the A_g mode is forbidden with the $Q_{\mathrm{R}}Q_{\mathrm{IR}_1}Q_{\mathrm{IR}_2}$ term because the product of two different odd irreps cannot equal the trivial irrep. For example, if phonons with the irreps B_{2u} and B_{3u} of a material with the point group mmm are pumped simultaneously, only Raman-active modes with the irrep B_{1g} can nonlinearly couple to them because $B_{1g} \subseteq B_{2u} \otimes B_{3u}$. For the quartic term $Q_{\mathrm{R}}^2Q_{\mathrm{IR}}^2$, any Raman mode can couple to the pumped mode because the square of any irrep is the trivial irrep.

After the nonlinear coefficients present in the polynomial fit of the calculated energy surface as a function of phonon coordinates are extracted, the phonons are treated as classical oscillators to study their light-induced dynamics. The coupled equations of motion for phonon coordinates are numerically solved in the presence of a forcing term of the form $F(t) = Z_\alpha^* F_0 \sin(\Omega t)\mathrm{e}^{-t^2/\sigma^2}$. Here, Z_α^* is the component of the mode effective charge along the direction α, and it is related to the Born effective charge tensor $Z_{\kappa,\alpha\beta}^*$ of atom κ with mass m_κ and the eigendisplacement vector

$w_{\kappa,\beta}$ by the expression $Z^*_\alpha = \Sigma_{\kappa,\beta} Z^*_{\alpha\beta} w_{\kappa,\beta}/\sqrt{m_\kappa}$ [26]. The mode effective charge can be calculated from first principles and is related to the LO–TO splitting that can be experimentally measured. Hence, except for the damping of the phonon modes that are roughly 10–20% of the respective phonon frequencies, all the quantities necessary for calculating the light-induced dynamics can be determined from first principles.

3. Coherent lattice displacement due to cubic-order coupling

3.1. *Coherent displacement in $Pr_{0.7}Ca_{0.3}MnO_3$*

An insulator–metal transition in $Pr_{0.7}Ca_{0.3}MnO_3$ after an excitation with a mid-IR laser was reported by Rini *et al.* in 2007 [20]. This was the first report of a pump–probe experiment in a transition metal oxide using a mid-IR pump that could excite the high-frequency IR-active phonons of the material causing changes in the metal-oxygen bond distances. The observed insulator–metal transition was understood in terms of the modification of the electronic bandwidth associated with the changes in these bond distances. In 2012, Först *et al.* proposed that nonlinear phonon coupling of the type $Q_R Q_{IR}^2$ can cause a coherent lattice displacement along the Raman-active phonon coordinate Q_R when the IR-active phonon coordinate Q_{IR} is externally pumped [13]. Subedi *et al.* theoretically investigated whether this nonlinear phononics phenonmenon can explain the observed insulator–metal transition in $Pr_{0.7}Ca_{0.3}MnO_3$ and found that externally exciting an IR-active phonon mode of this material can cause a lattice displacement along a low-frequency Raman-active phonon coordinate [38].

Optical spectroscopy shows that there is an IR-active phonon mode with a large oscillator strength in this material at 573 cm^{-1} [50]. In their experiment, Rini *et al.* used a mid-IR laser with a frequency near 573 cm^{-1} to pump this highest-frequency IR-active phonon of the material. For computational efficiency, Subedi *et al.* studied this phenomenon on the parent compound $PrMnO_3$. They started by calculating the zone center phonon frequencies and eigenvectors of this material. The calculated frequencies of the three highest IR-active phonon modes are 633, 640, and 661 cm^{-1} with irreps B_{1u}, B_{2u}, and B_{3u}, respectively. Since the product of an irrep with itself is the trivial irrep A_g, any of the seven A_g phonon modes present in the material can couple with an IR-active mode with a cubic-order $Q_R Q_{IR}^2$ nonlinear coupling. The irreps of the pumped IR-active mode and the A_g mode that couples to the pumped mode was not reported in the experimental study [20]. So total energies $E(Q_R, Q_{IR})$ as a function of the Q_R and Q_{IR} coordinates were calculated for each pair of A_g and high-frequency IR-active phonon modes. The $A_g(9)$ and B_{1u} modes showed a large nonlinear coupling, and the calculated energy surface of this pair is shown in Figure 1 (bottom). The high-frequency B_{1u} mode involves changes in the bond length between the apical O and Mn of the MnO_6 octahedra. The $A_g(9)$ mode has a relatively low calculated frequency of 155 cm^{-1} and involves rotation of the MnO_6 octahedra about the c axis as shown in Figure 1 (top). The in-plane angle between the corner-shared octahedra become closer to 90° for positive values of the $A_g(9)$ coordinate, while the distortion increases for negative values.

The calculated energy surface between $A_g(9)$ and B_{1u} modes fits the following polynomial

$$\begin{aligned} E(Q_R, Q_{IR}) = {} & \tfrac{1}{2}\Omega_R^2 Q_R^2 + \tfrac{1}{2}\Omega_{IR}^2 Q_{IR}^2 + \tfrac{1}{3} a_3 Q_R^3 + \tfrac{1}{4} b_4 Q_{IR}^4 \\ & - \tfrac{1}{2} g Q_R Q_{IR}^2, \end{aligned} \tag{1}$$

with Q_R and Q_{IR} now denoting the coordinates of the $A_g(9)$ and B_{1u} modes, respectively. Since the pump-induced dynamics causes large displacements along the phonon coordinates, they can be regarded as classical oscillators. The effect of an external pump on the IR-active mode can be treated by the presence of a driving term $F(t) = F\sin(\Omega t)e^{-t^2/2\sigma^2}$, where F, σ, and Ω are the

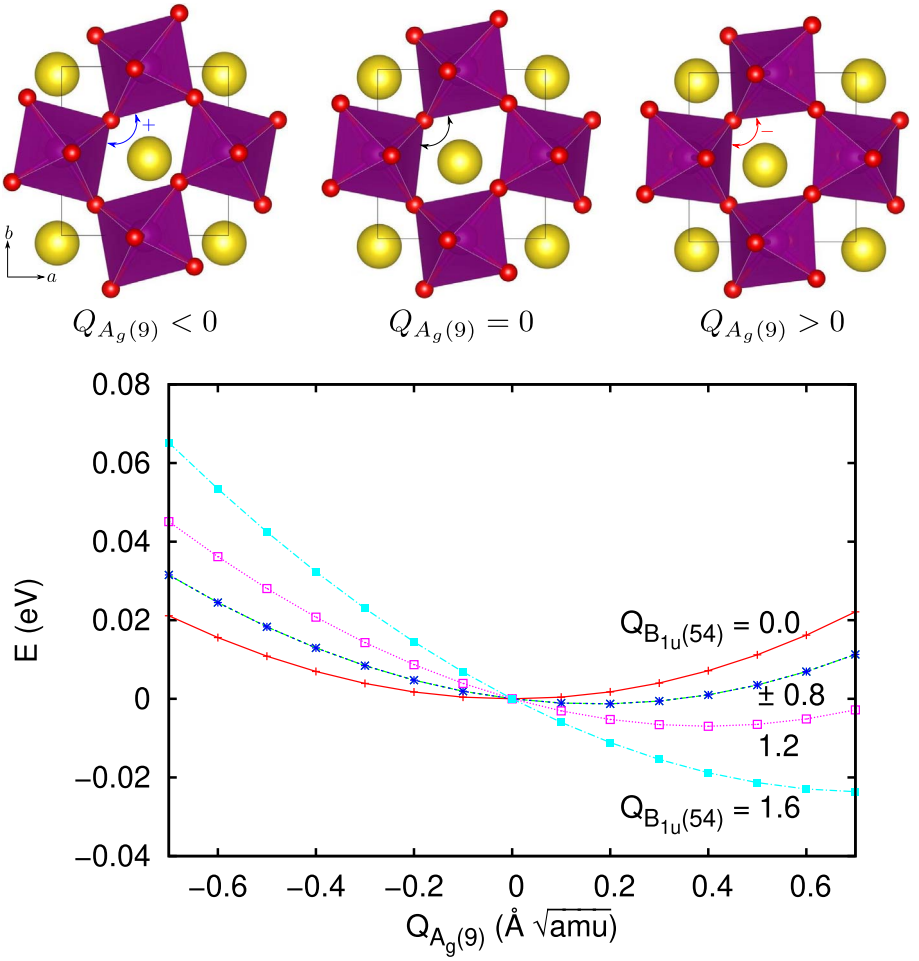

Figure 1. Top: sketch of the atomic displacements corresponding to the $A_g(9)$ Raman-active phonon mode of $PrMnO_3$ A positive value of the $A_g(9)$ coordinate brings the angle between octahedra closer to 90°. Bottom: total energy as a function of the $A_g(9)$ coordinate for several values of the B_{1u} coordinate. For visual clarity $E(Q_R, Q_{IR}) - E(0, Q_{IR})$ is plotted so that all curves coincide at $Q_R = 0$. Reproduced from [38].

amplitude, time-width and frequency of the pump pulse, respectively. The zero of the time delay t is typically chosen such that $t = 0$ when the pump and probe pulses are superposed. The coupled equations of motions for the two phonon coordinates in the absence of damping terms then read

$$\begin{aligned} \ddot{Q}_{IR} + \Omega_{IR}^2 Q_{IR} &= g Q_R Q_{IR} - b_4 Q_{IR}^3 + F(t) \\ \ddot{Q}_R + \Omega_R^2 Q_R &= \tfrac{1}{2} g Q_{IR}^2 - a_3 Q_R^2. \end{aligned} \tag{2}$$

For a finite pump amplitude F, the oscillation of the Q_{IR} coordinate has a time dependence $Q_{IR}(t) \propto F\Omega_{IR}\sigma^3 \cos\Omega_{IR} t$ [38]. Due to the cubic-order coupling between the two modes, the Raman coordinate experiences a forcing field $gQ_{IR}^2/2 \propto gF^2\Omega_{IR}^2\sigma^6(1 - \cos 2\Omega_{IR} t)$, which has a finite time-averaged value. Therefore, unlike the pumped IR-active mode, the Raman mode vibrates about a displaced position. Numerical solution of these coupled equations of motion also confirms this picture. Figures 2(a) and (b) show the dynamics of the Q_R coordinate with and

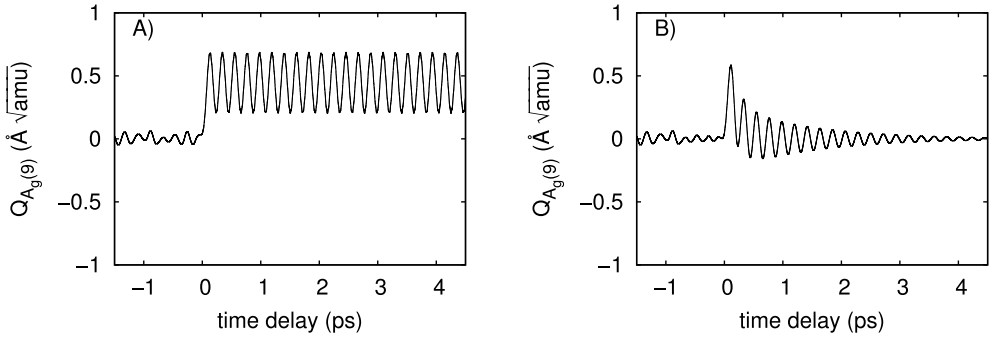

Figure 2. Dynamics of the $A_g(9)$ Raman mode. Left panel: dynamics without damping. Right panel: dynamics with damping values of 5% for both $A_g(9)$ and B_{1u} modes. Reproduced from [38].

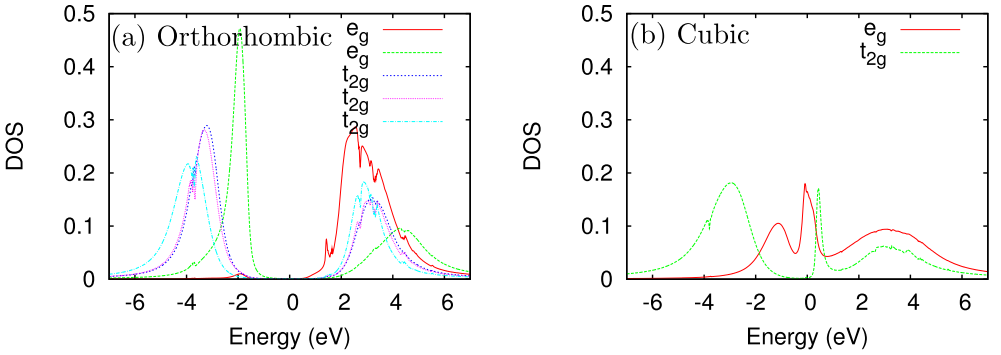

Figure 3. DFT+DMFT orbitally resolved density of states of Mn-d states in $PrMnO_3$ for the equilibrium orthorhombic (insulating) and cubic (metallic) crystal structures. Reproduced from [38].

without damping terms. In both cases, the Q_R coordinate oscillates about a displaced position while the Q_{IR} mode is also oscillating with a finite amplitude.

Since the lattice displaces along the positive value of the $A_g(9)$ coordinate while the B_{1u} is pumped, the rotation of the MnO_6 octahedra in the ab plane gets reduced. This should bring the system closer to the metallic phase because reduced octahedral rotation enhances hopping of the Mn d electrons via oxygen sites. Subedi *et al.* performed combined density functional theory and dynamical mean field theory (DMFT) electronic structure calculations on the cubic and equilibrium structures of $PrMnO_3$ to understand how the electronic structure changes as the octahedral rotation is suppressed. The calculated partial density of states of the Mn t_{2g} and e_g orbitals for the two structures are shown in Figure 3. They show that the distorted equilibrium structure is insulating, while the cubic structure is metallic. This suggests that light-induced suppression of the octahedral rotation due to nonlinear phononics might cause insulator–metal transition in this material.

Has it been conclusively shown that the observed mid-IR pump-induced insulator–metal transition in $Pr_{0.7}Ca_{0.3}MnO_3$ is due to displacement of the lattice along the Raman coordinate? It is worthwhile to point out that any magnetic, optical, and electrical perturbations easily cause insulator–metal transition in $Pr_{0.7}Ca_{0.3}MnO_3$ [51–53]. There have been no experiments to measure the oscillations of the pumped IR- and Raman-active modes using 2D spectroscopy to

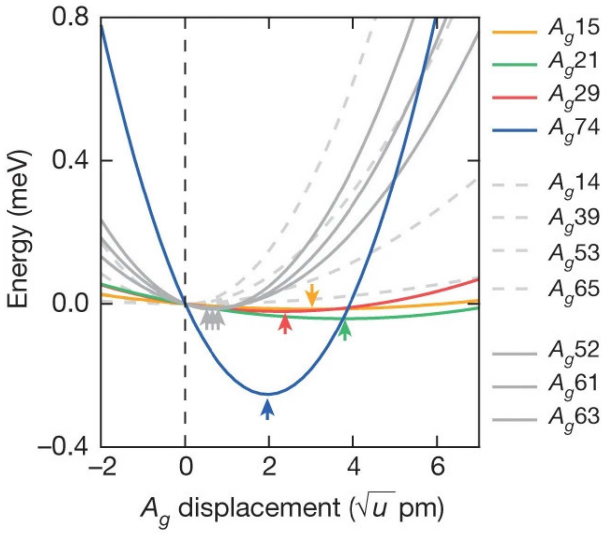

Figure 4. Calculated total energy of all the A_g modes for a frozen B_{1u} displacement of 0.14 Å $\sqrt{u}$ (u, atomic mass unit), corresponding to a change in the apical O–Cu distance of 2.2 pm. Arrows indicate the potential minima. Reproduced from [18].

show that these phonons are excited in the experiment, nor have the light-induced changes in the structure been studied using time-resolved X-ray diffraction spectroscopy. Moreover, since the light-induced transition is from an insulating to a metallic phase, heating effects cannot be ruled out as the cause of the transition unless the timescale for thermal redistribution of the pumped vibrational energy is disentangled from the timescale of any displacement along the Raman coordinate. As a result, it may be practically impossible to conclusively prove that pump-induced insulator–metal transition in this material is due to a displacement along the Raman coordinate.

3.2. *Coherent displacement in ortho-II $YBa_2Cu_3O_{6.5}$*

A mid-IR pump-induced increase in reflectivity has been observed in several cuprates, and this fact from raw data has been interpreted as a signature of light-induced transient superconductivity [29–31]. Mankowsky *et al.* have performed a combined time-resolved X-ray diffraction and first-principles lattice dynamics study to find out if the light-induced effect observed in $YBa_2Cu_3O_{6.5}$ is due to structural changes caused by nonlinear phononics [18]. Optical spectroscopy experiments show that this material has an IR-active phonon with a frequency of 640 cm^{-1} [54]. This mode has the irrep B_{1u}. Mankowsky *et al.* pumped this mode with an intense mid-IR laser pulse and measured changes in the diffraction intensity of four Bragg peaks as a function of time using time-resolved X-ray diffraction experiment. The intensities either increased or decreased promptly after a mid-IR pump. Since the intensity of a Bragg peak is proportional to the square of the structure factor, which is a function of atomic positions, this implies that the crystal structure of the material coherently changes after the pump. However, ortho-II $YBa_2Cu_3O_{6.5}$ has 25 atoms, and they were not able to fully resolve the light-induced changes in the crystal structure by measuring the changes in intensities of only four Bragg peaks.

There are 11 A_g modes in this material, and all of them can couple to the pumped B_{1u} mode with a cubic-order $Q_R Q_{IR}^2$ coupling. Mankowsky *et al.* calculated the total energy surface for each

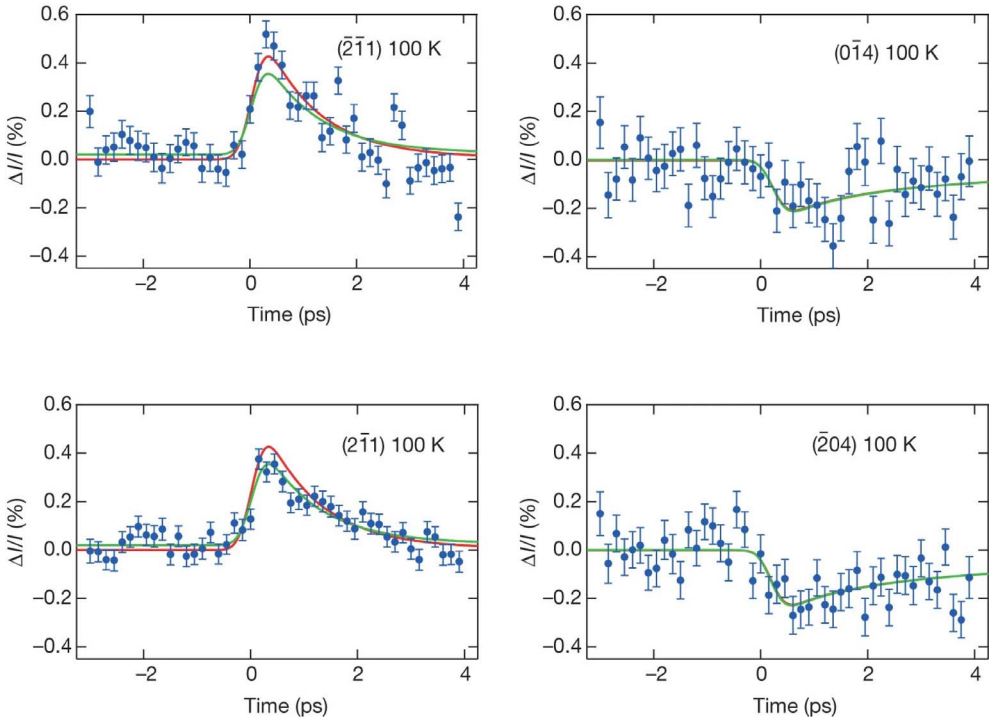

Figure 5. Time-dependent diffracted peak intensity (I) for four Bragg reflections. The solid curves are fit to the experimental data which were done by adjusting the B_{1u} amplitude and relaxation times. The relative amplitudes and signs of the curves are determined from the calculated structure using only the four most strongly coupled modes (green) or all A_g modes (red). Reproduced from [18].

pair of B_{1u} and A_g modes. The total energies of the seven A_g modes for a B_{1u} displacement of 0.14 Å $\sqrt{\text{amu}}$ are shown in Figure 4. The calculated energy curves show that four A_g modes show significant coupling to the pumped B_{1u} mode, and these modes involve out-of-plane motion of the apical O and Cu ions. The rest of the A_g modes that are weakly coupled involve in-plane motions of the O ions in the CuO_2 plane. The presence of these nonlinearities was also independently confirmed by the calculations of Ref. [55]. Changes in the intensities of the four Bragg peaks measured in the time-resolved X-ray diffraction experiment were calculated considering the displacement of the lattice along these A_g coordinates. The measured and calculated changes in the intensities of the Bragg peaks as a function of time are shown in Figure 5. With only the B_{1u} pump amplitude and the decay time as the fitting parameters, the changes in the crystal structure due to displacement along the A_g coordinates could independently reproduce the pump-induced changes in intensities of the four measured Bragg peaks. In the transient structure corresponding to the B_{1u} amplitude of 0.3 Å $\sqrt{\text{amu}}$ estimated for the pump intensity utilized in the the experiment, the apical O–Cu distance decreases and the O–Cu–O buckling increases. There is also an increase of the intra-bilayer distance and a decrease of the inter-bilayer distance. The changes in the distances are around 1 pm, and DFT calculations show that these cause practically no modification of the electronic structure for the estimated pump-induced amplitude of the B_{1u} mode in the experiment [18]. This suggests that structural changes due to nonlinear phononics do not cause the observed light-induced enhancement of reflectivity in this material.

3.3. *Excitation of Raman modes with nontrivial irreps in $ErFeO_3$*

$ErFeO_3$ is an insulator with a band gap of 2.1 eV, and it shows resonances at 540 and 567 cm^{-1} in the optical conductivity spectra corresponding to phonons with irreps B_{3u} and B_{2u}, respectively [56]. When either the B_{3u} or B_{2u} mode of this material was externally pumped with light polarized along a or b axes, respectively, Nova *et al.* observed oscillations at the frequency of 112 cm^{-1} corresponding to an A_g Raman-active phonon mode [14]. This reflects the cubic-order $Q_R Q_{IR}^2$ coupling between the pumped IR-active and A_g modes. In addition, they measured two B_{1g} phonons with frequencies of 112 and 162 cm^{-1} when the B_{3u} and B_{2u} modes were simultaneously pumped. The excitation of the B_{1g} phonons is due to a cubic-order $Q_{B_{1g}} Q_{B_{2u}} Q_{B_{3u}}$ coupling that is allowed by symmetry because $B_{1g} \subseteq B_{2u} \times B_{3u}$. Juraschek *et al.* studied the dynamics of these phonons in $ErFeO_3$ using theoretical framework described above and found large symmetry-allowed cubic-order couplings between the Raman- and IR-active phonons that explains the observed pump-induced Raman oscillations [39].

The observation of stimulated oscillations of Raman phonons due to nonlinear phonon couplings in $ErFeO_3$ is interesting because the band gap of this material is large enough that the role of electronic excitations in causing the light-induced dynamics can reasonably be ruled out. The observation of Raman oscillations at only two frequencies also raises an interesting question. Why are not the oscillations of other Raman A_g and B_{1g} modes observed? It can be conjectured that the respective nonlinear couplings are small or that the energy from the pumped IR modes flows mostly to low frequency Raman modes. It would be illuminating to perform experimental and theoretical studies that can clarify this issue. It would also be interesting to perform time-resolved X-ray diffraction experiment to find out whether the lattice displaces along the Raman-active phonon coordinates after a mid-IR pump in this material.

3.4. *Transient switching of ferroelectricity*

Although the capability to pump the IR-active phonons of transition metal oxides has been available since 2007 [20], a mechanism for switching ferroelectric order using nonlinear phononics was not discussed until 2015 [19]. The main reason for this delay in tackling this problem was a conceptual misunderstanding. Since the 1970s, nonlinear phonon couplings had been discussed in terms of ionic Raman scattering where excited IR-active phonons couple to Raman phonons via $Q_R Q_{IR}^2$ or $Q_R Q_{IR_1} Q_{IR_2}$ couplings [11, 12]. In centrosymmetric crystals, only Raman-active phonons, which do not break inversion symmetry, can couple to IR-active phonons at this order. Because the atomic displacement pattern associated with a ferroelectric order parameter derives from an unstable IR-active phonon, lattice displacements that change the ferroelectric order parameter via nonlinear phononics was not explored. In 2015, Subedi pointed out that any phonon mode Q_P that modifies the ferroelectric polarization is both Raman and IR active due to the lack of inversion symmetry in ferroelectric materials [19]. Thus, a cubic-order coupling is allowed between Q_P and any IR-active phonon that can be externally pumped. The question is whether the coupling is large and causes displacement along the direction that switches the ferroelectric order. This question was answered in the affirmative for the case of $PbTiO_3$.

The displacement patterns of the lowest (Q_P) and highest (Q_{IR}) frequency phonon modes of $PbTiO_3$ are shown in Figure 6 (top). The calculated total energy as a function of the Q_P coordinate for several values of the Q_{IR} coordinate is shown in Figure 6 (bottom). The minimum of the energy curve for the Q_P coordinate shifts towards the switching direction for both positive and negative values of the Q_{IR} coordinate, which reflects the presence of a $Q_P Q_{IR}^2$ nonlinear coupling term. There is an asymmetry in energy as a function of the Q_P coordinate because of the presence of a large Q_P^3 anharmonicity. Due to this anharmonic term, the minimum of

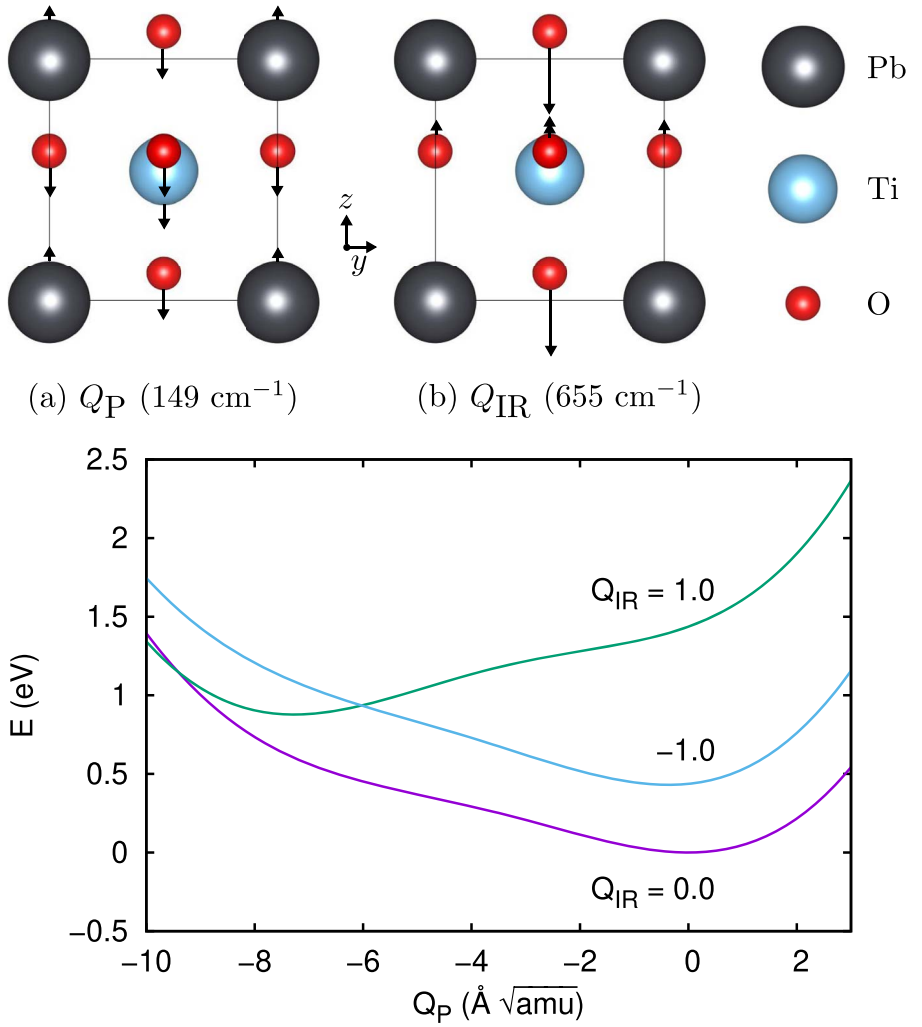

Figure 6. Top: displacement patterns of (a) lowest-frequency Q_{P} and (b) highest-frequency Q_{IR} modes of the ferroelectric phase of $PbTiO_3$. Bottom: total energy as a function of the Q_{P} coordinate for several values of the Q_{IR} coordinate. Reproduced from [19].

the Q_{P} coordinate suddenly jumps to a large negative when the value of the Q_{IR} coordinate is continuously increased to large positive values. This causes an abrupt reversal of the ferroelectric polarization without the magnitude of the polarization getting reduced to a value of zero. This phenonmena is seen in the numerical solutions of the coupled equations of motions for the Q_{P} and Q_{IR} coordinates in the presence of an external pump on the Q_{IR} mode as shown in Figure 7.

The phenomenon of light-induced switching of ferroelectrics via nonlinear phononics proposed by theory was partially confirmed by Mankowsky *et al.* [16]. They performed time-resolved measurements of SHG intensity and phase of an 800 nm probe pulse after a mid-IR excitation in $LiNbO_3$ with a pump duration of 150 fs. Their result is shown in Figure 8. For pump fluences smaller than 50 mJ/cm^2, the SHG intensity decreased to a finite value before returning to the equilibrium value. Above a threshold fluence of 60 mJ/cm^2, the intensity vanished completely,

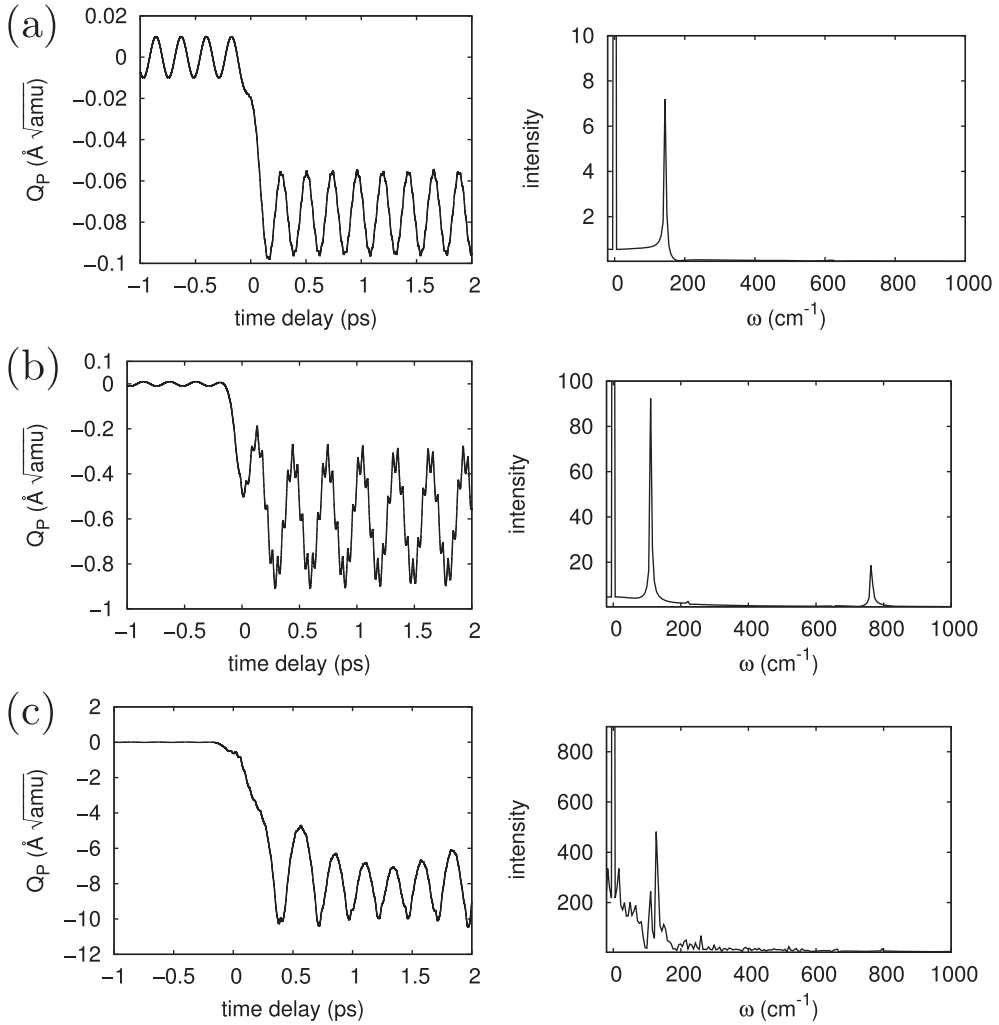

Figure 7. Dynamics of the Q_P mode for three different pump amplitudes. Left panels: displacements along Q_P coordinate as function of time delay. Right panels: Fourier transform of the positive time delay oscillations. Damping effects have been neglected. Reproduced from [19].

increased to a finite value, vanished completely again, and then relaxed to the equilibrium value. Their measurement of the phase of the second-harmonic signal showed that the phase changed by 180° whenever the SHG intensity vanished completely, which implies a temporary and partial reversal of the ferroelectric polarization. Furthermore, as can be seen in Figure 8, the SHG intensity also showed small modulations corresponding to the oscillations of the pumped IR-active phonon, and this indicates that the IR-active phonon is coherently oscillating while the polarization reversal is taking place. The state with switched polarization lasted only for 200 fs. Similar experiments with longer pump pulses are necessary to ascertain whether the switching lasts for the duration of the pump pulse or the pump only causes large-amplitude oscillations of the Q_P coordinate. In any case, even though Mankowsky *et al.* were not able to permanently switch the electric polarization, their experiment confirms the theoretical prediction that a cubic-order

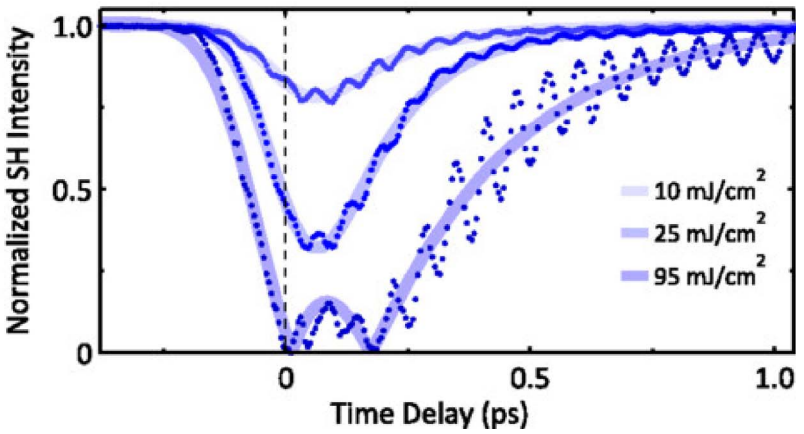

Figure 8. Time-resolved second-harmonic intensity of $LiNbO_3$ after a mid-IR pump. The intensity is normalized to its value before excitation. Reproduced from [16].

nonlinear phonon coupling with a large magnitude and an appropriate sign exists in oxide ferroelectrics that can reverse the electric polarization.

4. Symmetry breaking due to quartic coupling

4.1. *Quartic coupling between a Raman and an IR phonon modes*

Only cubic nonlinearities between phonon modes were discussed in the literature prior to 2014. This was presumably because higher order nonlinearities were thought to be small when the total energy of a crystal is expanded as a function of phonon coordinates. Subedi *et al.* pointed out that quartic nonlinearities between two phonon modes can be large when cubic nonlinearity is not allowed by symmetry [38]. In fact, a $Q_R^2 Q_{IR}^2$ term is the lowest order nonlinearity allowed by symmetry when Q_R has a non-trivial irrep.

Such a large quartic order coupling was found in La_2CuO_4 between its $B_{1g}(18)$ and $B_{3u}(41)$ phonon modes [38]. The $B_{1g}(18)$ mode changes the in-plane rotations of the CuO_6 octahedra as shown in Figure 9 (top), and the $B_{3u}(41)$ mode involves in-plane stretching of the Cu–O bonds. The $B_{1g}(18)$ mode breaks the m_x and m_y mirror symmetries. Therefore, the structures generated by the positive and negative values of the $B_{1g}(18)$ coordinates are related by these symmetries, and the total energy is symmetric as a function of the $B_{1g}(18)$ coordinate. Similarly, the $B_{3u}(41)$ mode breaks the m_z and inversion symmetries, and the total energy is also symmetric as a function of the $B_{3u}(41)$ coordinate.

The calculated total energy surface as a function of the $B_{1g}(18)$ and $B_{3u}(41)$ coordinates is shown in Figure 9 (bottom). It fits the expression

$$E(Q_R, Q_{IR}) = \tfrac{1}{2}\Omega_R^2 Q_R^2 + \tfrac{1}{2}\Omega_{IR}^2 Q_{IR}^2 + \tfrac{1}{4} a_4 Q_R^4 + \tfrac{1}{4} b_4 Q_{IR}^4 - \tfrac{1}{2} g Q_R^2 Q_{IR}^2, \quad (3)$$

where Q_R and Q_{IR} denote the coordinates of the $B_{1g}(18)$ and $B_{3u}(41)$ modes, respectively. As expected, the calculated energy surface is even with respect to both $B_{1g}(18)$ and $B_{3u}(41)$ coordinates, which is in contrast to the $Q_R Q_{IR}^2$ nonlinearity that is even only with respect to the IR phonon coordinate. The energy curve of the $B_{1g}(18)$ coordinate softens as the value of the $B_{3u}(41)$ coordinate is increased, and it develops a double well beyond a threshold value of the $B_{3u}(41)$ coordinate. In (3), this is reflected by a positive value of the coupling coefficient g.

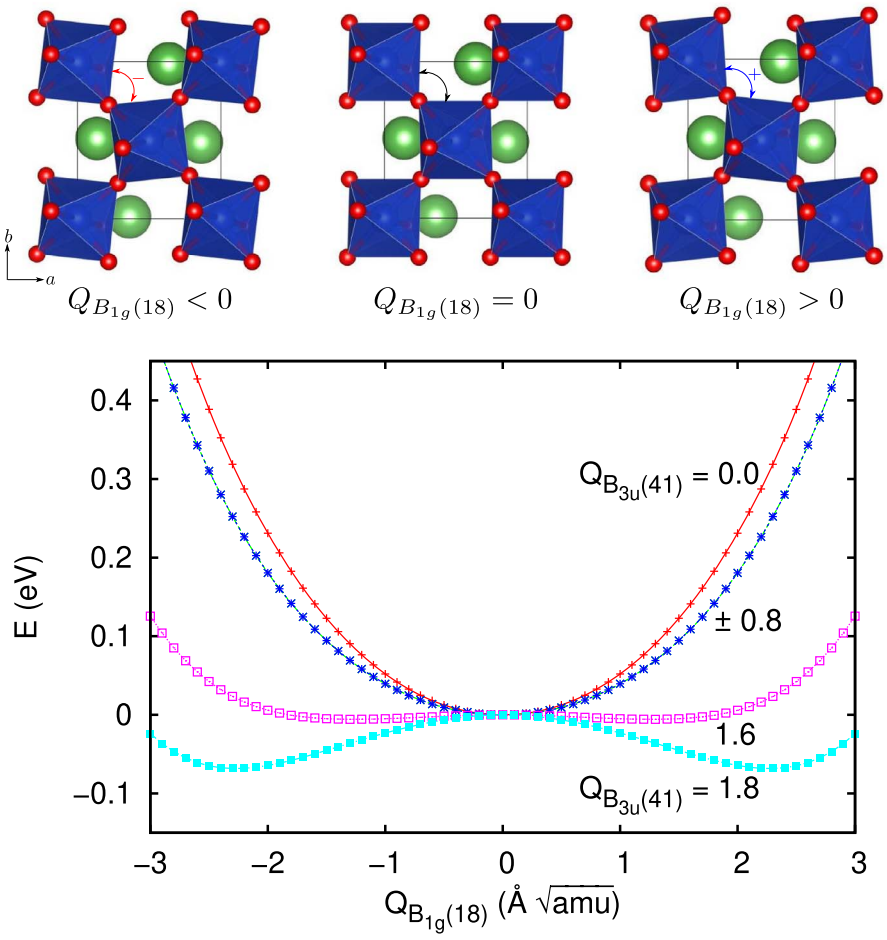

Figure 9. Top: sketch of the atomic displacements corresponding to the $B_{1g}(18)$ Raman-active phonon mode of La_2CuO_4. Bottom: total energy as a function of the $B_{1g}(18)$ coordinate for several values of the $B_{3u}(41)$ coordinate. For visual clarity $E(Q_R, Q_{IR}) - E(0, Q_{IR})$ is plotted so that all curves coincide at $Q_R = 0$. Reproduced from [38].

Since a finite value of the $B_{3u}(41)$ coordinate decreases the curvature of the energy curve of the $B_{1g}(18)$ coordinate, this implies that frequency of the $B_{1g}(18)$ mode changes while the $B_{3u}(41)$ is coherently oscillating. Furthermore, the $B_{1g}(18)$ mode should oscillate at a displaced position at one of the local minima of the double-well potential beyond a critical value of the amplitue of $B_{3u}(41)$ mode. This picture was confirmed by solving the coupled equations of motion of these modes, which are

$$\begin{aligned} \ddot{Q}_{IR} + \Omega_{IR}^2 Q_{IR} &= g Q_R^2 Q_{IR} - b_4 Q_{IR}^3 + F(t) \\ \ddot{Q}_R + \Omega_R^2 Q_R &= \tfrac{1}{2} g Q_R Q_{IR}^2 - a_4 Q_R^3. \end{aligned} \tag{4}$$

Here $F(t) = F \sin(\Omega t) e^{-t^2/2\sigma^2}$ is the external pump term on the $B_{3u}(41)$ coordinate, and F, σ, and Ω are the amplitude, width and frequency of the pump light pulse, respectively. Numerical solutions of these equations revealed four qualitatively different behavior for the oscillations of the $B_{1g}(18)$ mode, as depicted in Figure 10. The Raman mode oscillates about its local minimum below a threshold value F_c of the external pump (Figure 10(a)). Near this threshold,

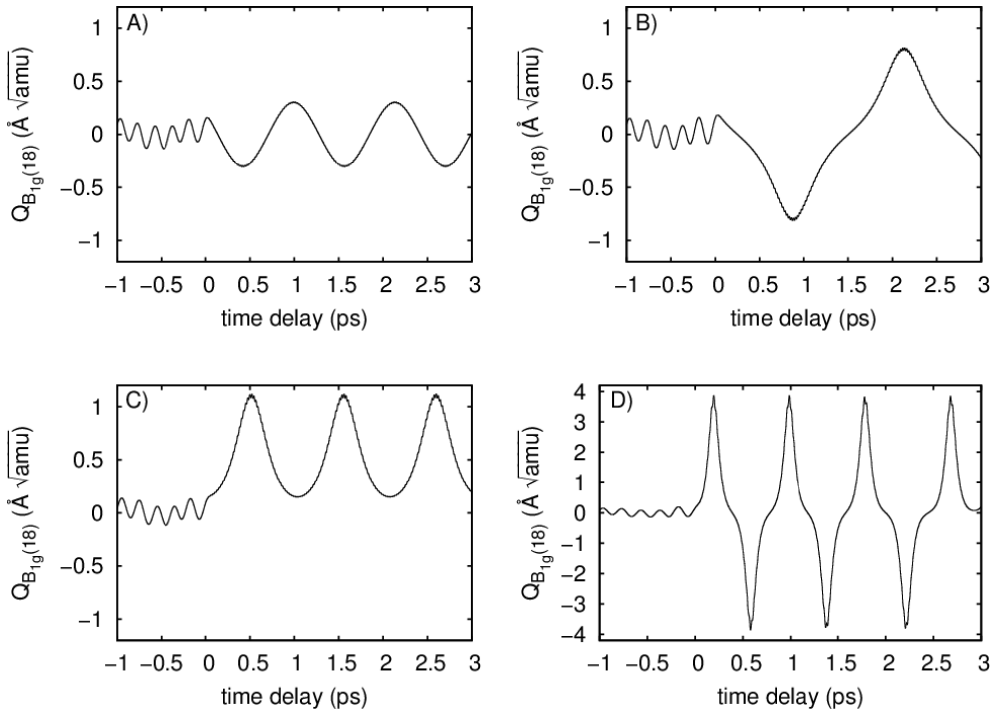

Figure 10. Dynamics of the $B_{1g}(18)$ coordinate due to a quartic nonlinearity in La_2CuO_4. Damping effects have been neglected. Reproduced from [38].

there is a narrow range where it makes a long period oscillation about the local maximum of the double well potential, which is analogous to the Kapitza phenomenon for a vibrating pendulum (Figure 10(b)). As the pump amplitude is increased further, it oscillates at a displaced position in one of the minima of the double well (Figure 10(c)). At even larger values of the pump amplitude, it again oscillates about the equilibrium position with a large amplitude that encompasses both minima of the double well potential (Figure 10(d)).

Since $B_{1g}(18)$ mode breaks the m_x and m_y mirror symmetries, the oscillations about the displaced position in Figure 10(c) describe a light-induced dynamical symmetry breaking of the crystal. This is a non-perturbative effect that occurs above a critical threshold of the pump field. Although intense pump pulses with peak fields greater than 10 MV/cm are available these days, experimental studies of this phenomenon in La_2CuO_4 have not yet been reported in the literature.

4.2. *Light induced ferroelectricity due to quartic coupling between two IR phonon modes*

Quartic nonlinearities of the type $Q_1^2 Q_2^2$ are allowed by symmetry between any two phonon coordinates Q_1 and Q_2 because the square of an irrep is the trivial irrep. Therefore, two IR-active phonon modes can also couple with each other. Subedi showed that such a nonlinearity can lead to transiently induced ferroelectricity in strained $KTaO_3$ [26]. This phenomenon was illustrated for the case of 0.6% compressively strained $KTaO_3$ by studying the dynamics of its two lowest-frequency IR-active phonons when its highest-frequency IR-active phonon mode is pumped. The two lowest-frequency phonon modes in this system have the irreps A_{2u} and E_u. The A_{2u} mode with calculated frequency $\Omega_{l_z} = 20$ cm^{-1} involves atomic motions along the z axis, whereas the

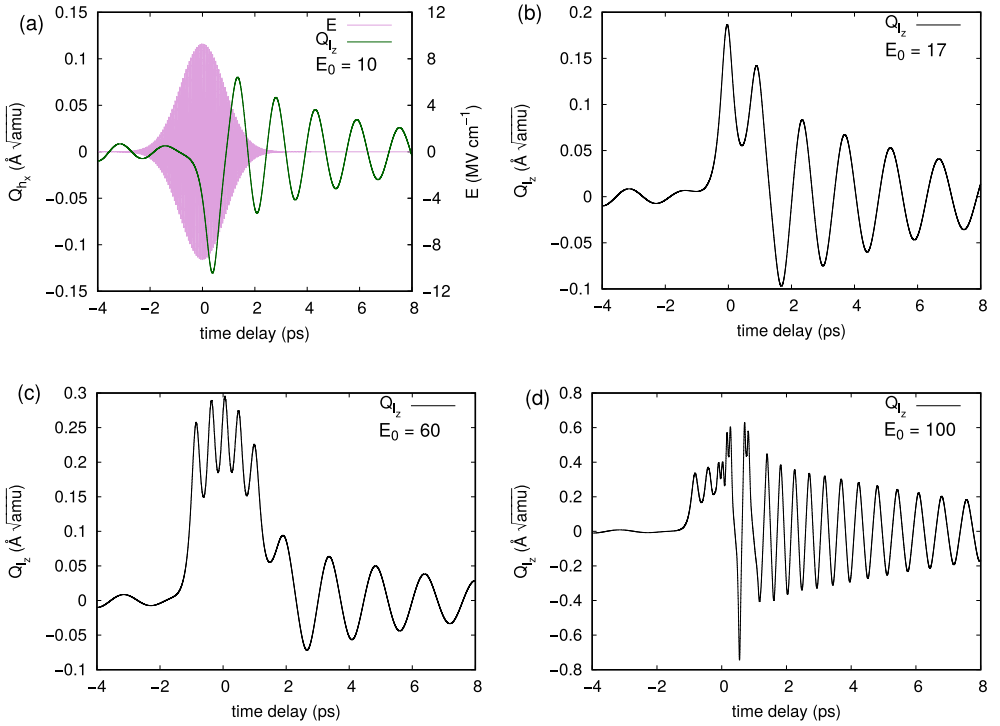

Figure 11. Dynamics of the Q_{l_z} coordinate of strained $KTaO_3$ after Q_{h_x} coordinate has been pumped by an external pulse E with duration of 2 ps. The dynamics for four different values of the peak electric field E_0 (MV·cm^{-1}) of the pump pulse are shown. Damping effects are taken into account in this study. Reproduced from [26].

doubly degenerate E_u mode with frequency $\Omega_{l_x} = \Omega_{l_y} = 122$ cm^{-1} causes the atoms to move in the xy plane. The highest-frequency mode that should be pumped to induce ferroelectricity has the irrep E_u with frequency $\Omega_{h_x} = \Omega_{h_y} = 556$ cm^{-1}.

Total energy calculations as a function of the phonon coordinates showed that the highest-frequency mode couples to the two lowest-frequency modes in this system with large quartic nonlinearities. The coupling is such that the energy curve of the low-frequency E_u coordinate Q_{l_x} stiffens, whereas the energy curve of the low-frequency A_u coordinate Q_{l_z} softens when the highest-frequency coordinate Q_{h_x} has a finite value. The calculated total energies as a function of these three coordinates were fit to a polynomial. These coordinates were treated as classical oscillators, and the fitted polynomial was used as their potential energy. The coupled equations of motion in the presence of an external pump were numerically solved for several values of pump intensities, and four such solutions for the Q_{l_z} coordinate is shown in Figure 11. Similar to the case of $Q_R^2 Q_{IR}^2$ coupling in La_2CuO_4 discussed in the previous section, here also the lowest-frequency Q_P coordinate oscillates about a local minimum above a pump threshold (Figures 11(b) and (c)). Since the displacement along the Q_P coordinate breaks inversion symmetry, these calculations show that light-induced ferroelectricity can be stabilized due to the $Q_P^2 Q_{IR}^2$ nonlinear coupling.

Nova *et al.* have pumped the highest-frequency IR-active phonon of paraelectric $SrTiO_3$ [27]. They did not observe any second harmonic signal of an optical probe pulse from the sample after it was pumped by a single mid-IR pulse, indicating that the sample remained paraelectric after the mid-IR pump. However, when the sample was exposed to a mid-IR pump for several minutes, the formation of a metastable ferroelectric state was inferred from a finite second harmonic

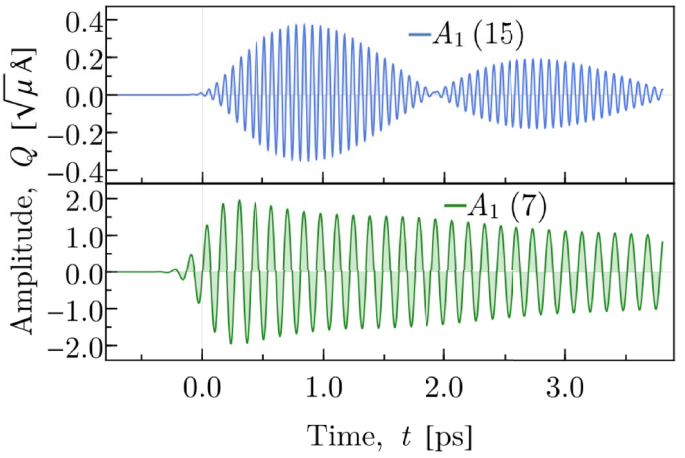

Figure 12. Dynamics of the high-frequency Q_{IR_2} coordinate (denoted by $A_1(15)$) after the low-frequency Q_{IR_1} coordinate (denoted by $A_1(7)$) is externally pumped. Reproduced from [57].

signal of the probe pulse. The metastable ferroelectric state persisted for several hours after being exposed to the mid-IR irradiation. Intriguingly, similar metastable ferroelectric state was obtained by using teraherz pump [28]. This suggests that nonlinear phononics may not be the cause of transient ferroelectricity in the experiment of Nova *et al.*

5. Phonon upconversion due to ionic Raman scattering

Majority of the experimental and theoretical investigations of the nonlinear phononics phenomena have focused on pumping the high-frequency IR-active phonons of materials to induce dynamics along their low-frequency phonon modes. Juraschek and Maehrlein proposed that a phenomenon analogous to sum frequency Raman scattering can occur due to a $Q_{\mathrm{IR}_1}Q^2_{\mathrm{IR}_2}$ nonlinearity in a material with two IR-active phonons with the relation $\Omega_{\mathrm{IR}_1} = \Omega_{\mathrm{IR}_2}/2$ [57]. They found that when the low-frequency coordinate Q_{IR_1} is resonantly pumped, the cubic nonlinearity can cause oscillations of the high-frequency coordinate Q_{IR_2}.

They considered the simplest form of nonlinear lattice potential $V(Q_{\mathrm{IR}_1}, Q_{\mathrm{IR}_2}) = (1/2)\Omega^2_{\mathrm{IR}_1}Q^2_{\mathrm{IR}_1} + (1/2)\Omega^2_{\mathrm{IR}_2}Q^2_{\mathrm{IR}_2} + cQ_{\mathrm{IR}_1}Q^2_{\mathrm{IR}_2}$. This leads to the coupled equations of motions

$$\begin{aligned} \ddot{Q}_{\mathrm{IR}_1} + \gamma_{\mathrm{IR}_1}\dot{Q}_{\mathrm{IR}_1} + (\Omega^2_{\mathrm{IR}_1} + 2cQ_{\mathrm{IR}_2})Q_{\mathrm{IR}_1} &= Z_{\mathrm{IR}_1}E(t), \\ \ddot{Q}_{\mathrm{IR}_2} + \gamma_{\mathrm{IR}_2}\dot{Q}_{\mathrm{IR}_2} + \Omega^2_{\mathrm{IR}_2}Q_{\mathrm{IR}_2} &= cQ^2_{\mathrm{IR}_1}(t). \end{aligned} \tag{5}$$

Here, γ_{IR_1} and γ_{IR_2} describe the damping of the Q_{IR_1} and Q_{IR_2} coordinates, respectively, and Z_{IR_1} denotes the mode effective charge of the low-frequency Q_{IR_1} coordinate. The results of numerical solutions of these equations in the presence of a finite driving field $E(t)$ with frequency $\omega_0 = \Omega_{\mathrm{IR}_1}$ is shown in Figure 12, which shows the high-frequency Q_{IR_2} mode oscillating due to sum-frequency upconversion.

Kozina *et al.* have experimentally demonstrated this phenomenon in $SrTiO_3$ [58]. When they pumped the lowest-frequency transverse optic TO_1 phonon of this material, they also observed lattice oscillations at higher frequencies corresponding to the transverse optic TO_2 and TO_3 modes in time-resolved X-ray diffraction experiments. The TO_1 mode has a frequency of 1.5–2.5 THz depending on the sample temperature, whereas the TO_2 and TO_3 modes have frequencies of 5.15 and 7.6 THz, respectively. This indicates that the phonon upconversion mechanism

proposed by Juraschek and Maehrlein works even when the frequencies of the high-frequency phonon modes are not integer multiples of the frequency of the pumped low-frequency phonon mode.

6. Control of magnetism via nonlinear phononics

6.1. *Magnon excitation via nonlinear magneto-phonon coupling in $ErFeO_3$*

$ErFeO_3$ is an antiferromagnetic insulator with a small residual ferromagnetic moment that arises due to a canting associated with the Dzyaloshinskii–Moriya interaction. Earlier in this review, the observation of the A_g and B_{1g} phonon modes after a mid-IR pump by Nova *et al.* was discussed [14]. Interestingly, they also observed oscillations corresponding to a low-frequency magnon when the B_{2u} and B_{3u} IR-active phonons were simultaneously excited. The B_{2u} and B_{3u} modes are polarized along the b and a axes, respectively. Since a finite value of their respective coordinates Q_{2u} and Q_3u leads to a formation of finite electrical dipole moments along the b and a axes, respectively, simultaneous excitation of these modes using a circularly polarized pulse should give rise to circulating charges inside the lattice. Nova *et al.* proposed that this generates an effective magnetic field that excites the low-frequency magnon. Their scenario has been supported by a microscopic theory based on first principles calculations [59].

6.2. *Modifying the magnetic state of a material*

Nonlinear phononics can coherently modify atomic distances inside a crystal. In magnetic materials, this can also alter exchange interactions, and a modified magnetic state might get stabilized in the light-induced transient state. Fechner *et al.* have theoretically proposed that the equilibrium antiferromagnetic ordering of Cr_2O_3 gets modified to another antiferromagnetic ordering with ferromagnetically coupled nearest-neighbor spins when its high-frequency IR-active phonon mode with the irrep A_u is externally pumped [60]. This occurs because the Cr–Cr distances increase in the transient state as a result of the displacement along an A_g Raman mode due to a $Q_{\mathrm{R}}Q_{\mathrm{IR}}^2$ nonlinearity. Similar modification of the equilibrium magnetic state to a hidden antiferromagnetic state has been proposed in the rare-earth titantes by Gu and Rondinelli [61] and Khalsa and Benedek [62].

More interestingly, Radaelli has proposed that ferroelectricity and ferromagnetism can be induced in piezoelectric and piezomagnetic materials, respectively, by simultaneously pumping the orthogonal components Q_{IR}^x and Q_{IR}^y of a doubly degenerate IR-active mode with the irrep E_u [40]. The metastable states occur because the simultaneous pumping of the orthogonal components causes a displacement along a Raman-active phonon mode with a nontrival irrep due to a $Q_{\mathrm{R}}^{xy}Q_{\mathrm{IR}}^xQ_{\mathrm{IR}}^y$ nonlinearity. It was shown that the displacement along the Raman coordinate Q_{R}^{xy}, which transforms as xy, is given by

$$\begin{aligned} Q_{\mathrm{IR}}^{xy} &\propto 2Q_{\mathrm{IR,max}}^xQ_{\mathrm{IR,max}}^y\cos\Delta\phi \\ &\propto 2E_xE_y\cos\Delta\phi. \end{aligned} \tag{6}$$

Here $Q_{\mathrm{IR,max}}^x$ and $Q_{\mathrm{IR,max}}^y$ are the amplitudes of the Q_{IR}^x and Q_{IR}^y modes, respectively. E_x and E_y are the magnitudes of the electric fields used to pump the Q_{IR}^x and Q_{IR}^y modes, respectively, and $\Delta\phi$ is their phase difference. Because the displacement along the Q_{IR}^{xy} coordinate is proportional to $\cos\Delta\phi$, Q_{IR}^{xy} has a finite value only when the orthogonal components of E_u are pumped in-phase or out-of-phase. Furthermore, the displacement along Q_{R}^{xy} coordinate switches direction wherever the phase difference changes by π. Thus, the $Q_{\mathrm{R}}^{xy}Q_{\mathrm{IR}}^xQ_{\mathrm{IR}}^y$ nonlinearity can induce ferroelectricity or ferromagnetism if the ferroelectric polarization or ferromagnetic moment is proportional to the Q_{R}^{xy} coordinate, and the direction of the induced ferroelectric or ferromagnetic

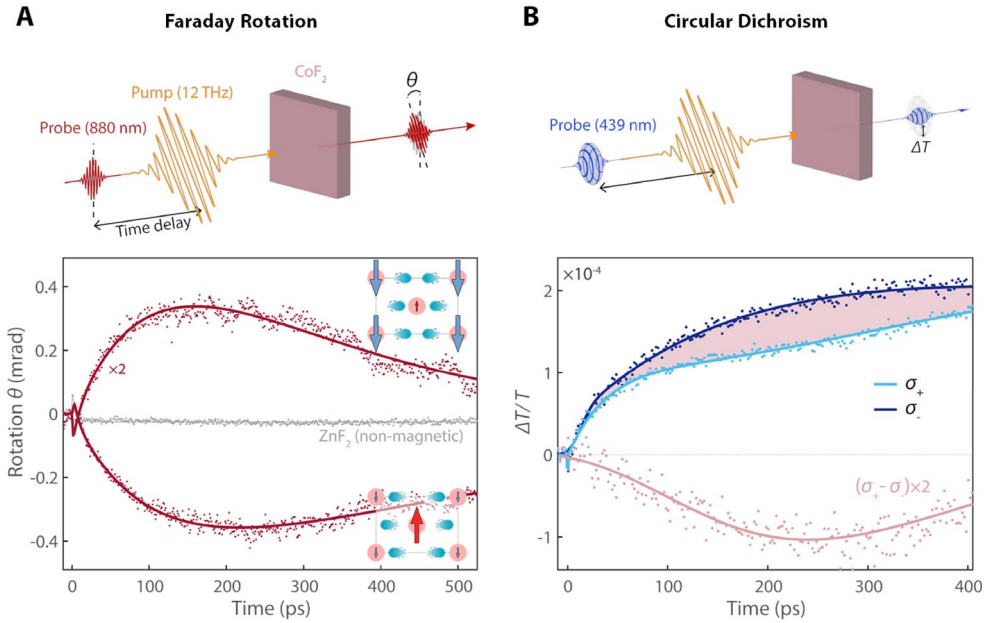

Figure 13. A (top): Depiction of mid-IR pump-Faraday rotation probe setup. A (bottom): Faraday rotation in CoF_2 after a 12 THz pump for two polarizations of the pump pulses (+45° and −45°. B (top): Depiction of mid-IR pump-circular dichroism probe setup. B (bottom): The relative change in transmission for left (dark blue) and right (light blue) circular polarized probe pulses. Reproduced from [42].

moment can be controlled by changing the phase difference of the pump pulse. Radaelli has suggested that peizoelectric BPO_4 and piezomagnetic CoF_2 are candidate materials where this type of ferroelectricity and ferromagnetism can be induced, respectively, using nonlinear phononics.

Disa *et al.* have recently demonstrated this phenomena in CoF_2 [42]. This material is a compensated antiferromagnet below $T_N = 39$ K, and an application of a strain along the [110] direction induces a ferrimagnetic state with a finite magnetic moment. They were able to stabilize a similar ferrimagnetic state by simultaneously pumping the orthogonal components of its high-frequency IR-active phonon with the irrep E_u, which should displace the lattice along a Raman-active phonon with the irrep B_{2g} due to the $Q_{\mathrm{R}}^{xy} Q_{\mathrm{IR}}^{x} Q_{\mathrm{IR}}^{y}$ nonlinearity. A displacement along the B_{2g} mode causes one set of Co–F distances in the material to lengthen while Co–F distances in another sublattice shortens, and this is responsible for the uncompensation of Co moments. The presence of a finite net magnetic moment in the transient state was confirmed by time-resolved measurements of the Faraday rotation and circular dicroism of probe pulses. As shown in Figure 13, a pump-induced magnetic signal was immediately observed, which changed sign after 7 ps. After the sign reversal, the magnetic signal continued to grow until it reached its maximum value at 200 ps. The reason for such a long-lived magnetic signal has not been completely understood. One possibility proposed by Disa *et al.* is that the transient displacement along the Raman-active phonon coordinate is reinforced by induced magnetic moment. Time-resolved X-ray diffraction studies should help in understanding this long-lived metastable state by clarifying the nature of the structural distortions in the light-induced phase. In particular, oscillations and displacements along the B_{2g} coordinate should be observed while the Q_{IR}^{x} and Q_{IR}^{y} coordinates are simultaneously oscillating to confirm that the transient ferrimagnetism is due to nonlinear phononics.

7. Conclusions

In summary, nonlinear phononics is an emerging field that has the potential to develop as a powerful method for controlling materials by stabilizing novel crystal structures that cannot be accessed in equilibrium. This is made possible by coherent atomic displacements along a set of phonon coordinates after a selective excitation of the IR-active phonons of a material, and it contrasts with the incoherent atomic motions that result from heating. Nonlinear coupling of the pumped IR-active phonon to other phonons is the microscopic mechanism responsible for the coherent lattice displacement. Intense mid-IR pump pulses are now available, and mid-IR light-induced control of materials properties have been demonstrated in pump–probe experiments. Nevertheless, this field is still in infancy compared to the pump–probe experimental activities that are performed in chemistry laboratories. 2D pump–probe spectroscopy experiments are routinely used by chemists to directly observe simultaneous excitations of the pumped vibrational mode as well as other modes that are excited due to nonlinear couplings. The nonlinearity between different vibrational modes are reflected by the presence of off-diagonal signals in 2D spectroscopy, and they can be used to quantify the nonlinear couplings. Mid-IR pump-second harmonic probe experiments similar to 2D spectroscopy have been recently performed on the wide band gap insulator $LiNbO_3$, and they have demonstrated simultaneous oscillations of the pumped IR-active mode while the lattice gets displaced along a Raman-active phonon coordinate. Several mid-IR pump induced phase transitions have been attributed to coherent lattice displacements due to nonlinear phononics, including insulator–metal transitions and melting of spin and orbital orders. Mid-IR pump-induced increase in reflectivity have also been reported in several superconductors, and they have been interpreted as signatures of light-enhanced superconductivity. However, excitations of the pumped mode have not been experimentally demonstrated in these experiments. More experimental studies that directly measure the nonlinear phonon couplings between the pumped phonon and other active phonon degrees of freedom would put this field on a stronger footing.

A microscopic theory based on first principles calculations of nonlinear phonon couplings has been developed to study the dynamics of a material when its IR-active phonons are selectively pumped. In addition to the cubic nonlinearities discussed in the 1970s, quartic nonlinearities with large coupling coefficients that can stabilize a symmetry-broken phase beyond a threshold value of the pump intensity has been found using this theoretical approach. Theoretical studies have also proposed light-induced reversal of ferroelectric polarization, ferroelectricity in paraelectrics and ferromagnetism in antiferromagnets, and these predictions have been partially confirmed by experiments. Cavity control of nonlinear couplings and phono-magneto analog of opto-magneto effect have been shown to be feasible by calculations. Their experimental realizations would confirm that nonlinear phononics is truly a novel way to control the physical properties of materials.

Acknowledgements

I am grateful to Antoine Georges and Andrea Cavalleri for previous collaborations on this subject. I have also benefited from helpful discussions with Michael Först, Roman Mankowsky, Tobia Nova, Matteo Mitrano, Srivats Rajasekaran and Yannis Laplace on this topic.

References

[1] A. H. Zewail, “Laser selective chemistry — is it possible?”, *Phys. Today* **33** (1980), p. 27-33.
[2] R. N. Zare, “Laser control of chemical reactions”, *Science* **279** (1998), no. 5358, p. 1875-1879.

[3] W. S. Warren, H. Rabitz, M. Dahleh, "Coherent control of quantum dynamics: The dream is alive", *Science* **259** (1993), p. 1581-1589.
[4] N. Bloembergen, A. H. Zewail, "Energy redistribution in isolated molecules and the question of mode-selective laser chemistry revisited", *J. Phys. Chem.* **88** (1984), p. 5459-5465.
[5] C. S. Parmenter, "Vibrational redistribution within excited electronic states of polyatomic molecules", *Faraday Discuss. Chem. Soc.* **75** (1983), p. 7-22.
[6] D. J. Nesbitt, R. W. Field, "Vibrational energy flow in highly excited molecules: Role of intramolecular vibrational redistribution", *J. Phys. Chem.* **100** (1996), p. 12735-12756.
[7] S. Woutersen, P. Hamm, "Nonlinear two-dimensional vibrational spectroscopy of peptides", *J. Phys. Condens. Matter* **14** (2002), no. 39, article no. R1035–R1062.
[8] M. Khalil, A. Tokmakoff, "Signatures of vibrational interactions in coherent two-dimensional infrared spectroscopy", *Chem. Phys.* **266** (2001), p. 213-230.
[9] M. Khalil, N. Demirdöven, A. Tokmakoff, "Coherent 2D IR spectroscopy: Molecular structure and dynamics in solution", *J. Phys. Chem.* **107** (2003), p. 5258-5279.
[10] N. Huse, K. Heyne, J. Dreyer, E. T. J. Nibbering, T. Elsaesser, "Vibrational multilevel quantum coherence due to anharmonic couplings in intermolecular hydrogen bonds", *Phys. Rev. Lett.* **91** (2003), article no. 197401.
[11] R. F. Wallis, A. A. Maradudin, "Ionic Raman effect. II. The first-order ionic Raman effect", *Phys. Rev. B* **3** (1971), p. 2063-2075.
[12] T. P. Martin, L. Genzel, "Ionic Raman scattering and ionic frequency mixing", *Phys. Status Solidi B* **61** (1974), no. 2, p. 493-502.
[13] M. Först, C. Manzoni, S. Kaiser, Y. Tomioka, Y. Tokura, R. Merlin, A. Cavalleri, "Nonlinear phononics as an ultrafast route to lattice control", *Nat. Phys.* **7** (2011), p. 854-866.
[14] T. F. Nova, A. Cartella, A. Cantaluppi, M. Först, D. Bossini, R. V. Mikhaylovskiy, A. V. Kimel, A. Cavalleri, "An effective magnetic field from optically driven phonons", *Nat. Phys.* **13** (2016), p. 132-136.
[15] J. R. Hortensius, D. Afanasiev, A. Sasani, E. Bousquet, A. D. Caviglia, "Ultrafast strain engineering and coherent structural dynamics from resonantly driven optical phonons in $LaAlO_3$", *NPJ Quant. Mater.* **5** (2020), article no. 95.
[16] R. Mankowsky, A. von Hoegen, M. Först, A. Cavalleri, "Ultrafast reversal of the ferroelectric polarization", *Phys. Rev. Lett.* **118** (2017), article no. 197601.
[17] M. Först, R. Mankowsky, H. Bromberger, D. M. Fritz, H. Lemke, D. Zhu, M. Chollet, Y. Tomioka, Y. Tokura, R. Merlin, J. P. Hill, S. L. Johnson, A. Cavalleri, "Displacive lattice excitation through nonlinear phononics viewed by femtosecond X-ray diffraction", *Solid State Commun.* **169** (2013), p. 24-27.
[18] R. Mankowsky, A. Subedi, M. Först, S. O. Mariager, M. Chollet, H. T. Lemke, J. S. Robinson, J. M. Glownia, M. P. Minitti, A. Frano *et al.*, "Nonlinear lattice dynamics as a basis for enhanced superconductivity in $YBa_2Cu_3O_{6.5}$", *Nature (London)* **516** (2014), p. 71-73.
[19] A. Subedi, "Proposal for ultrafast switching of ferroelectrics using midinfrared pulses", *Phys. Rev. B* **92** (2015), article no. 214303.
[20] M. Rini, R. Tobey, N. Dean, J. Itatani, Y. Tomioka, Y. Tokura, R. W. Schoenlein, A. Cavalleri, "Control of the electronic phase of a manganite by mode-selective vibrational excitation", *Nature (London)* **449** (2007), p. 72-74.
[21] V. Esposito, M. Fechner, R. Mankowsky, H. Lemke, M. Chollet, J. M. Glownia, M. Nakamura, M. Kawasaki, Y. Tokura, U. Staub, P. Beaud, M. Först, "Nonlinear electron–phonon coupling in doped manganites", *Phys. Rev. Lett.* **118** (2017), article no. 247601.
[22] A. D. Caviglia, R. Scherwitzl, P. Popovich, W. Hu, H. Bromberger, R. Singla, M. Mitrano, M. C. Hoffmann, S. Kaiser, P. Zubko *et al.*, "Nonlinear electron–phonon coupling in doped manganites", *Phys. Rev. Lett.* **108** (2012), article no. 136801.
[23] R. I. Tobey, D. Prabhakaran, A. T. Boothroyd, A. Cavalleri, "Ultrafast electronic phase transition in $La_{1/2}Sr_{3/2}MnO_4$ by coherent vibrational excitation: Evidence for nonthermal melting of orbital order", *Phys. Rev. Lett.* **101** (2008), article no. 197404.
[24] M. Först, R. I. Tobey, S. Wall, H. Broberger, V. Khanna, A. L. Cavalieri, Y.-D. Chuang, W. S. Lee, R. Moore, W. F. Schlotter *et al.*, "Driving magnetic order in a manganite by ultrafast lattice excitation", *Phys. Rev. B* **84** (2011), article no. 241104(R).
[25] M. Först, A. D. Caviglia, R. Scherwitzl, R. Mankowsky, P. Zubko, V. Khanna, H. Bromberger, S. B. Wilkins, Y.-D. Chuang, W. S. Lee *et al.*, "Spatially resolved ultrafast magnetic dynamics initiated at a complex oxide heterointerface", *Nat. Mater.* **14** (2015), p. 883-888.
[26] A. Subedi, "Midinfrared-light-induced ferroelectricity in oxide paraelectrics via nonlinear phononics", *Phys. Rev. B* **95** (2017), article no. 134113.
[27] T. F. Nova, A. S. Disa, M. Fechner, A. Cavalleri, "Metastable ferroelectricity in optically strained $SrTiO_3$", *Science* **364** (2019), p. 1075-1079.
[28] X. Li, T. Qiu, J. Zhang, E. Baldini, J. Lu, A. M. Rappe, K. A. Nelson, "Terahertz field-induced ferroelectricity in quantum paraelectric $SrTiO_3$", *Science* **364** (2019), p. 1079-1082.

[29] D. Fausti, R. I. Tobey, N. Dean, S. Kaiser, A. Dienst, M. C. Hoffmann, S. Pyon, T. Takayama, H. Takagi, A. Cavalleri, "Light-induced superconductivity in a stripe-ordered cuprate", *Science* **331** (2011), p. 189-191.
[30] S. Kaiser, C. R. Hunt, D. Nicoletti, W. Hu, I. Gierz, H. Y. Liu, M. Le Tacon, T. Loew, D. Haug, B. Keimer, A. Cavalleri, "Optically induced coherent transport far above Tc in underdoped $YBa_2Cu_3O_{6+\delta}$", *Phys. Rev. B* **89** (2014), article no. 184516.
[31] W. Hu, S. Kaiser, D. Nicoletti, C. R. Hunt, I. Gierz, M. C. Hoffmann, M. Le Tacon, T. Loew, B. Keimer, A. Cavalleri, "Optically enhanced coherent transport in $YBa_2Cu_3O_{6.5}$ by ultrafast redistribution of interlayer coupling", *Nat. Mater.* **13** (2014), p. 705-711.
[32] M. Mitrano, A. Cantaluppi, D. Nicoletti, S. Kaiser, A. Perucchi, S. Lupi, P. Di Pietro, D. Pontiroli, M. Ricc, S. R. Clark, D. Jaksch, A. Cavalleri, "Possible light-induced superconductivity in K_3C_{60} at high temperature", *Nature (London)* **530** (2016), p. 461-464.
[33] R. Mankowsky, M. Först, A. Cavalleri, "Non-equilibrium control of complex solids by nonlinear phononics", *Rep. Prog. Phys.* **79** (2016), article no. 064503.
[34] D. Nicoletti, A. Cavalleri, "Nonlinear light-matter interaction at terahertz frequencies", *Adv. Opt. Photon. 8* (2016), p. 401-464.
[35] A. Cavalleri, "Photo-induced superconductivity", *Contemp. Phys.* **59** (2018), p. 31-46.
[36] T. Qi, Y.-H. Shin, K.-L. Yeh, K. A. Nelson, A. M. Rappe, "Collective coherent control: Synchronization of polarization in ferroelectric $PbTiO_3$ by shaped THz fields", *Phys. Rev. Lett.* **102** (2009), article no. 247603.
[37] Y. Shinohara, K. Yabana, Y. Kawashita, J.-I. Iwata, T. Otobe, G. F. Bertsch, "Coherent phonon generation in time-dependent density functional theory", *Phys. Rev. B* **82** (2010), article no. 155110.
[38] A. Subedi, A. Cavalleri, A. Georges, "Theory of nonlinear phononics for coherent light control of solids", *Phys. Rev. B* **89** (2014), article no. 220301(R).
[39] D. M. Juraschek, M. Fechner, N. A. Spaldin, "Ultrafast structure switching through nonlinear phononics", *Phys. Rev. Lett.* **118** (2017), article no. 054101.
[40] P. G. Radaelli, "Breaking symmetry with light: Ultrafast ferroelectricity and magnetism from three-phonon coupling", *Phys. Rev. B* **97** (2018), article no. 085145.
[41] D. Afanasiev, J. R. Hortensius, B. A. Ivanov, A. Sasani, E. Bousquet, Y. M. Blanter, R. V. Mikhaylovskiy, A. V. Kimel, A. D. Caviglia, "Ultrafast control of magnetic interactions via light-driven phonons", *Nat. Mater.* (2021), p. 1-5.
[42] A. S. Disa, M. Fechner, T. F. Nova, B. Liu, M. Först, D. Prabhakaran, P. G. Radaelli, A. Cavalleri, "Polarizing an antiferromagnet by optical engineering of the crystal field", *Nat. Phys.* **16** (2020), p. 937-941.
[43] M. Gu, J. M. Rondinelli, "Ultrafast band engineering and transient spin currents in antiferromagnetic oxides", *Sci. Rep.* **6** (2016), article no. 25121.
[44] D. M. Juraschek, P. Narang, N. A. Spaldin, "Phono-magnetic analogs to opto-magnetic effects", *Phys. Rev. Res.* **2** (2020), article no. 043035.
[45] D. M. Juraschek, T. Neuman, J. Flick, P. Narang, "Cavity control of nonlinear phononics", https://arxiv.org/abs/1912.00122, 2019.
[46] D. M. Juraschek, Q. N. Meier, P. Narang, "Parametric excitation of an optically silent Goldstone-like phonon mode", *Phys. Rev. Lett.* **124** (2020), article no. 117401.
[47] M. Först, R. Mankowsky, A. Cavalleri, "Mode-selective control of the crystal lattice", *Acc. Chem. Res.* **48** (2015), p. 380-387.
[48] M. Buzzi, M. Först, A. Cavalleri, "Measuring non-equilibrium dynamics in complex solids with ultrashort X-ray pulses", *Phil. Trans. R. Soc. A* **377** (2019), no. 2145, article no. 20170478.
[49] P. Salén, M. Basini, S. Bonetti, J. Hebling, M. Krasilnikov, A. Y. Nikitin, G. Shamuilov, Z. Tibai, V. Zhaunerchyk, V. Goryashko, "Matter manipulation with extreme terahertz light: Progress in the enabling THz technology", *Phys. Rep.* **836-837** (2019), p. 1-74.
[50] Y. Okimoto, Y. Tomioka, Y. Onose, Y. Otsuka, Y. Tokura, "Optical study of $Pr_{1-x}Ca_xMnO_3$ ($x = 0.4$) in a magnetic field: Variation of electronic structure with charge ordering and disordering phase transitions", *Phys. Rev. B* **59** (1999), p. 7401-7408.
[51] Y. Tomioka, A. Asamitsu, H. Kuwahara, Y. Moritomo, Y. Tokura, "Magnetic-field-induced metal-insulator phenomena in $Pr_{1-x}Ca_xMnO_3$ with controlled charge-ordering instability", *Phys. Rev. B* **53** (1996), article no. R1689–R1692.
[52] K. Miyano, T. Tanaka, Y. Tomioka, Y. Tokura, "Photoinduced insulator-to-metal transition in a perovskite manganite", *Phys. Rev. Lett.* **78** (1997), p. 4257-4260.
[53] A. Asamitsu, Y. Tomioka, H. Kuwahara, Y. Tokura, "Current switching of resistive states in magnetoresistive manganites", *Nature (London)* **388** (1997), p. 50-52.
[54] C. C. Homes, T. Timusk, D. A. Bonn, R. Liang, W. N. Hardy, "Optical properties along the c-axis of $YBa_2Cu_3O_{6+x}$, for $x = 0.50 \rightarrow 0.95$ evolution of the pseudogap", *Physica C* **254** (1995), no. 3-4, p. 265-280.
[55] M. Fechner, N. A. Spaldin, "Effects of intense optical phonon pumping on the structure and electronic properties of yttrium barium copper oxide", *Phys. Rev. B* **94** (2016), article no. 134307.

[56] G. V. Subba Rao, C. N. R. Rao, J. R. Ferraro, "Infrared and electronic spectra of rare earth perovskites: Ortho-chromites, -manganites and -ferrites", *Appl. Spectrosc.* **24** (1970), p. 436-445.
[57] D. M. Juraschek, S. F. Maehrlein, "Sum-frequency ionic Raman scattering", *Phys. Rev. B* **97** (2018), article no. 174302.
[58] M. Kozina, M. Fechner, P. Marsik, T. van Driel, J. M. Glownia, C. Bernhard, M. Radovic, D. Zhu, S. Bonetti, U. Staub, M. C. Hoffmann, "Terahertz-driven phonon upconversion in $SrTiO_3$", *Nat. Phys.* **15** (2019), p. 387-392.
[59] D. M. Juraschek, M. Fechner, A. V. Balatsky, N. A. Spaldin, "Dynamical multiferroicity", *Phys. Rev. Mater.* **1** (2017), article no. 014401.
[60] M. Fechner, A. Sukhov, L. Chotorlishvili, C. Kenel, J. Berakdar, N. A. Spaldin, "Magnetophononics: Ultrafast spin control through the lattice", *Phys. Rev. Mater.* **2** (2018), article no. 064401.
[61] M. Gu, J. M. Rondinelli, "Nonlinear phononic control and emergent magnetism in Mott insulating titanates", *Phys. Rev. B* **98** (2018), article no. 024102.
[62] G. Khalsa, N. A. Benedek, "Ultrafast optically induced ferromagnetic/anti-ferromagnetic phase transition in $GdTiO_3$ from first principles", *NPJ Quant. Mater.* **3** (2018), article no. 15.